



Drug Discovery–Development Interface

Repurposing the Pentameric B-Subunit of Shiga Toxin for Gb3-Targeted Immunotherapy of Colorectal Cancer by Rhamnose Conjugation



Zhicheng Liu^a, Xia Li^a, Zhongkai Lu^a, Xinfang Qin^a, Haofei Hong^a, Zhifang Zhou^a, Roland J. Pieters^b, Jie Shi^{a,*}, Zhimeng Wu^{a,*}

^a Key Laboratory of Carbohydrate Chemistry & Biotechnology, Ministry of Education, School of Biotechnology, Jiangnan University, 214122 Wuxi, China

^b Department of Chemical Biology & Drug Discovery, Utrecht Institute for Pharmaceutical Sciences, Utrecht University, Universiteitsweg 99, 3584 CG Utrecht, the Netherlands

ARTICLE INFO

Article history:

Received 27 March 2022

Revised 21 July 2022

Accepted 22 July 2022

Available online 26 July 2022

Key words:

Gb3

StxB

Rhamnose

Multivalency

Immunotherapy

Colorectal cancer

ABSTRACT

Globotriaosylceramide (Gb3 or CD77) is a tumor-associated carbohydrate antigen implicated in several types of cancer that serves as a potential cancer marker for developing target-specific diagnosis and therapy. However, the development of Gb3-targeted therapeutics has been challenging due to its carbohydrate nature. In the present work, taking advantage of its natural pentamer architecture and Gb3-specific targeting of shiga toxin B subunit (StxB), we constructed a pentameric antibody recruiting chimera by site-specifically conjugating StxB with the rhamnose hapten for immunotherapy of colorectal cancer. The Sortase A-catalyzed enzymatic tethering of rhamnose moieties to the C terminus of StxB had very moderate effect on their pentamer architectures and thus the resultant conjugates maintained the potent ability to bind to Gb3 antigen both immobilized on an assay plate and expressed on colorectal cancer cells. All StxB-rhamnose constructs were capable of efficiently mediating the binding of rhamnose antibodies onto HT29 colorectal cancer cells, which was further shown to be able to induce cancer cell lysis by eliciting potent antibody-dependent cellular cytotoxicity (ADCC) and complement-dependent cytotoxicity (CDC) *in vitro*. Finally, the best StxB-rhamnose conjugate, *i.e.* 1B-3R, was confirmed to be able to inhibit the colorectal tumor growth using a HT29-derived xenograft murine model. Taken together, our data demonstrated the potential of repurposing StxB as an excellent multivalent scaffold for developing Gb3-targeted biotherapeutics and StxB-rhamnose conjugates might be promising candidates for targeted immunotherapy of Gb3-related colorectal cancer.

© 2022 American Pharmacists Association. Published by Elsevier Inc. All rights reserved.

Introduction

Globotriaosylceramide (Gb3 or CD77) is a tumor-associated carbohydrate antigen of globo-series glycosphingolipid, and the increased expression of Gb3 has been found in a variety of tumor types including colorectal cancer,^{1–3} gastric cancer,⁴ pancreatic cancer,^{2,5} and breast cancer,⁶ therefore attracting extensive attempts to exploit Gb3 antigen for target-specific diagnosis and therapy. The development of therapeutic antibodies targeting Gb3 seems more difficult than for other carbohydrate antigens,^{7,8} possibly due to its low immunogenicity and the fact that a carbohydrate-specific antibody often matures with an affinity lower than that of a protein-specific antibody by several orders of magnitude.⁹ Thus, most attempts have been focused on exploiting natural Gb3 binding lectins, among

which the most attractive one is the B subunit of Shiga toxin (StxB). This toxin is associated with pathogens of shigella species and shiga toxin-expression *E. coli* (STEC).¹⁰ Without the disease-causing A subunit of Shiga toxin, the lectin part B (StxB) is non-toxic and also only weakly immunogenic. Moreover, StxB is likely more robust than antibodies in terms of binding affinity to Gb3. However, the specificity of an antibody may be superior to StxB, because StxB binds to Gb2¹¹ and Gb4 as well.^{12,13} Each individual monomer of StxB offers three distinct binding sites for Gb3 and the non-covalently associated homo-pentamer of StxB therefore can theoretically bind for up to fifteen Gb3 molecules with an affinity that falls into the nanomolar range, thus representing an excellent example of the power of multivalency in nature. The feasibility of using StxB as a tumor-specific moiety has been well demonstrated in the constructions of immunotoxins,¹⁴ intracellular drug delivery carriers^{13,15} and as an imaging reagent.¹⁶ Recently, StxB binding potential to colorectal tumor was also demonstrated in a genetic porcine model.¹⁷

* Corresponding authors.

E-mail addresses: j.shi@jiangnan.edu.cn (J. Shi), z.wu@jiangnan.edu.cn (Z. Wu).

Antibody-recruiting molecules are a group of bifunctional chimeras intended for passive cancer immunotherapy by indirectly utilizing disease-irrelevant antibodies existing naturally in the human blood, such as the endogenous antibodies against L-rhamnose, dinitrophenol, and α -Gal.^{18,19} A hapten of an endogenous antibody as the antibody-binding ligand can be covalently conjugated to a tumor antigen-specific ligand to form a typical antibody-recruiting molecule, which can selectively localize at the tumor site with concomitant recruitment of the endogenous antibodies for immune effector functions including antibody-dependent cellular cytotoxicity (ADCC), complement-dependent cytotoxicity (CDC), and antibody-dependent phagocytosis (ADCP). The effect of an antibody-recruiting molecule can be significantly augmented by introducing multivalency mechanisms,²⁰ which has been well established by displaying multiple tumor antigen-specific ligands and/or antibody-binding ligands on liposomes,²¹ lipid polymers,^{22,23} glycopolymers²⁴ and peptide scaffolds.²⁵ Multivalency is a ubiquitous organization format of molecules involved in the biological systems especially for interactions between ligands and receptors, which offers a low affinity ligand an opportunity to establish an association to its counter receptor with high affinity and sensitivity in its multivalent form and vice versa. Thus, introducing the multivalency concept to antibody-recruiting molecules enables the exploration of natural carbohydrate-binding lectins as promising tumor antigen-specific ligands.

In this work, we report the construction, *in vitro* and *in vivo* evaluation of a novel antibody-recruiting molecule made of the pentameric StxB conjugated site specifically with the rhamnose hapten for Gb3-specific immunotherapy of colorectal cancer. The enzymatic tethering of multiple rhamnose modules to Stx1B and Stx2B only had a moderate effect on their pentameric architecture as the conjugates maintained the potent ability to bind to the Gb3 antigen on surface both of an assay plate and colorectal HT29 cancer cells. All the constructs were capable of efficiently mediating binding of rhamnose antibodies and eliciting strong ADCC and CDC on HT29 colorectal cancer cells *in vitro*. The best one StxB-rhamnose conjugate 1B-3R was shown to be able to inhibit the tumor growth in a HT29 colorectal cancer cell-derived xenograft tumor murine model. Taken together, our data demonstrated the potential use of StxB as an excellent multivalent scaffold to develop antibody-recruiting molecule or similar multivalent therapeutics against cancer.

Materials and Methods

Materials

The *E. coli* plasmids encoding Stx1B (pET22b-Stx1B) and Stx2B (pET22b-Stx2B) were constructed with optimized codons by General Biosystems company (Anhui, China). The Nickel column (HisTrap HP) for protein purification and HiPrep desalting column were provided by Jincheng Biological company (Wuhan, China). The FSL-Gb3 receptor was obtained from Sigma-Aldrich company (Shanghai, China). Cell culture medium including McCoy's 5A, RPMI 1640, and Dulbecco's Modified Eagle Medium (DMEM) were provided by GE Healthcare company (Shanghai, China). Antibiotics solution of Penicillin-Streptomycin and Fetal Bovine Serum (FBS) for cell culture was obtained from ThermoFisher Scientific company (Shanghai, China). Alexa Flour 488-labeled Goat anti-Rabbit IgG antibodies were bought from Proteintech company (Beijing, China) and Alexa Fluor 647-labeled Goat anti-Rabbit IgG antibodies were bought from Abcam company (Shanghai, China). The anti-rhamnose rabbit serum was prepared in our lab. Anti-Myc Rabbit Polyclonal antibodies, anti-His Rabbit Polyclonal antibodies, HRP-conjugated detection antibodies used in this work, LDH cytotoxicity kit, WST-8 kit, and other routine reagents were provided by Beyotime biotech company (Shanghai, China).

Cell Culture

Cancer cell lines including K562, Caco-2, Hela and HT29 were preserved and routinely cultured at our lab. K562 cells were cultured in RPMI 1640 medium. Caco-2 cells and Hela cells were cultured in DMEM medium. HT29 cells were cultured in McCoy's 5A medium. All the above medium was supplemented with FBS to 10% and antibiotics solution of penicillin (100 U/mL) and streptomycin (100 μ g/mL). The mycoplasma test was done routinely. All cell lines were grown in a cell culture incubator provided with humidified atmosphere of 5% CO₂ at 37°C.

StxB Expression and Purification

Competent cells of BL21(DE3) *E. coli* were transformed with the plasmids of pET22b-Stx1B and pET22b-Stx2B, respectively. The *E. coli* cells were then inoculated into Luria-Bertani medium supplemented with ampicillin and grown at 37°C at a shaking incubator. Once the OD₆₀₀ of above culture increased to 0.6–0.8, StxB protein expression was initiated by adding IPTG (0.1 mM) into the culture and protein production was allowed for 12 h at 16°C. The *E. coli* cells were then collected by centrifugation at 9000 rpm for 5 min and the resultant pellet was resuspended for further sonication-assisted cell lysis using a buffer containing 10 mM Tris-HCl, 300 mM NaCl, pH 7.4. The clear supernatant with recombinant StxB proteins was obtained after further centrifugation at 10,000 rpm for 20 min. The above supernatant was then transferred into the pre-equilibrated nickel affinity column (HisTrap HP) and purification was performed by following the manufacturer's protocol. The elution of StxB proteins was achieved through stepwise washing the column using elution buffers containing imidazole at concentrations from 100 mM to 500 mM, and eluted fractions were prepared in 1.5 mL tube for later SDS-PAGE validation. Confirmed proteins were pooled together and concentration was quantified through the BCA assay.

Sortase A-Catalyzed Rhamnose Conjugation of StxB

Rhamnose conjugation of StxB proteins (1B and 2B) was achieved by through a Sortase A-catalyzed site-specific enzymatic ligation as we reported previously.²⁶ The enzymatic reaction was initiated by mixing the rhamnose derivatives (500 μ M), 1B or 2B (15 μ M) and Sortase A (2 μ M) in a buffer of 50 mM Tris-HCl, 150 mM NaCl, and 5 mM CaCl₂, pH 7.5. The enzymatic reaction was allowed for 3 h at 16°C on a rotator. To purify the StxB-rhamnose conjugates, Sortase A and unreacted StxB proteins containing His tag were first removed out of the crude reaction through a reverse nickel affinity protein purification. The reaction solution was further purified by a molecular weight cutting off filter unit (3 kDa) to remove the excess rhamnose derivatives. The purified conjugates were then validated through SDS-PAGE analysis and western blotting as described in the corresponding context. The validated StxB-rhamnose conjugates were further filtered through a 0.22 μ M sterile filtration unit and protein concentrations were quantified through the BCA assay.

Western Blotting

The StxB-rhamnose conjugates was also characterized through western blotting analysis. The unmodified StxB proteins and StxB-rhamnose conjugates were first boiled in the protein loading buffer to prepare denatured samples. Electrophoretic separation of those samples was then achieved by using SDS-PAGE gel (12%). All proteins in the gel were next transferred onto methanol-activated PVDF membrane which was further blocked by a blocking buffer of 5% BSA-TBST solution for 2 h at 37°C. The membrane was then incubated with the corresponding primary antibodies overnight at 4°C as described in

the context and it was further probed with HRP-labeled goat anti-rabbit IgG detection antibodies for 2 h at 37°C. Finally, HRP-driven luminescence was generated by adding ECL reagent and images were recorded using a Gel Doc XR instrument (Bio-Rad).

Dynamic Lights Scattering (DLS) Analysis of the Conjugates

The effect of rhamnose conjugation on StxB protein pentameric structure was analyzed by comparing the size distribution of StxB-rhamnose conjugates with the parental StxB proteins using dynamic light scattering (DLS). The StxB-rhamnose conjugates were diluted at 10 μM in water and subjected to Zetasizer Nano ZS (Malvern Panalytical) for size distribution analysis. Stx1B-His was used as a reference pentameric protein for particle size, as it has been reported to function as a pentamer.²⁷ The collected data was analyzed with Zetasizer Software (Malvern Panalytical).

Gb3 Binding Assay

The Gb3 binding capability of StxB-rhamnose conjugates and StxB was compared by using an ELISA type assay with Gb3-immobilized as reported previously.¹¹ The FSL-Gb3 compound was dissolved by PBS to 2 $\mu\text{g}/\text{mL}$ and it was coated onto a 96-well plate with 100 $\mu\text{L}/\text{well}$ at 4°C overnight. Then, the coated plate was washed with 0.2% BSA-PBS to remove the unbound FLS-Gb3, and it was further blocked with 200 μL blocking buffer of 3% BSA-PBS at room temperature for 2 h. After washing the plate with 0.2% BSA-PBS, StxB-rhamnose conjugates (100 $\mu\text{L}/\text{well}$) or StxB (100 $\mu\text{L}/\text{well}$) at concentrations as mentioned in the context were added and the plate was further incubated for 2 h. Again, the plate was washed by 0.2% BSA-PBS, and 100 $\mu\text{L}/\text{well}$ of Myc-tag rabbit polyclonal antibodies (1 $\mu\text{g}/\text{mL}$) was added for further incubation for additional 1 h. After washing three times with 0.2% BSA-PBS, the plate was added with 100 $\mu\text{L}/\text{well}$ of HRP-conjugated goat anti-rabbit IgG (H+L) antibodies (1 $\mu\text{g}/\text{mL}$), and incubated for another 1 h. With final washing by using 0.2% BSA-PBS, each well of the plate was further added with 100 μL of TMB substrate. After about 10 min, the HRP enzymatic reaction was quenched by adding each well with 25 μL of H_2SO_4 (2 M), followed by reading the plate at 450 nm through iMark microplate absorbance reader (Bio-rad).

Flow Cytometry Analysis

The ability of StxB-Rhamnose conjugates to bind to Gb3 receptor and mediate the binding of rhamnose antibodies on cells was assessed by using flow cytometry-based assay. HT29 cells were diluted into flow cytometry buffer of 2% BSA-PBS to reach the concentration of 4.0×10^5 cells/mL. StxB-rhamnose conjugates or StxB proteins were mixed with 100 μL of the prepared cells (4.0×10^4) to a final concentration 500 nM and incubated at room temperature for 0.5 h. For conjugates binding analysis, 100 μL of Myc-tag rabbit polyclonal antibody (20 $\mu\text{g}/\text{mL}$) was then added into cells after brief washing cells with PBS and the mixture was incubated for 0.5 h. For the rhamnose antibody binding analysis, 100 μL of anti-rhamnose rabbit serum (1:50 dilution) was then added into cells after brief washing cells with PBS and the mixture was incubated for 0.5 h. With further washing using PBS, the treated cells were then resuspended in 100 μL of Alexa Fluor 647-labeled Goat Anti-Rabbit IgG antibodies (20 $\mu\text{g}/\text{mL}$) and incubated for 0.5 h. As a negative control, cells were treated with PBS to replace the conjugates. The treated cells were finally resuspended by 200 μL flow cytometry buffer after twice washing with PBS, and analysis was carried out on the Accuri C6 flow cytometer. Data processing was performed by using the FlowJo software.

Immunocytochemistry Assay

The rhamnose antibody binding capability of the StxB-rhamnose conjugates was also visualized by immunocytochemistry assay. HT29 cells with an initial density of 10^4 cells per well were cultured in a 96-well plate overnight. Following removal of the supernatant medium, a solution of 4% paraformaldehyde was added to fix the cells attached on the plate for about 10 min, and followed by blocking the plate through 3% BSA-PBS for additional 1 h. After three times washing with PBS, the cells were then incubated with StxB-rhamnose conjugates or StxB protein at a concentration of 500 nM and incubated for 1 h. After PBS washing, cells were further incubated with 100 μL of anti-rhamnose rabbit serum (1:250 dilution) for another 1 h. With washing three times using PBS, the cells were then incubated with 100 μL of Alexa Fluor 488-labeled Goat anti-rabbit IgG antibodies (4 $\mu\text{g}/\text{mL}$) for another 1 h. After three times washing by using PBS, the cells were finally stained by antifade mounting reagent containing 4',6-diamidino-2-phenylindole (DAPI). Labeled cells were imaged by using fluorescent microscopy.

ADCC Assay

The ADCC-specific tumor killing capability of the StxB-rhamnose conjugates was determined by using HT29 as target cancer cells and peripheral blood mononuclear cells (PBMC) as effector immune cells. HT29 cells with initial density of 10^4 cells/well were grown in a 96-well plate overnight. The cells attached on the plate were first incubated either with StxB-rhamnose conjugates (500 nM) or StxB protein (500 nM) in the presence of anti-rhamnose rabbit serum (1:50 dilution) at the incubator for 30 min. After brief washing of the plate, freshly isolated human PBMC were introduced into the plate with a ratio of PBMC to HT29 in 20:1, and the plate was then kept at the incubator for additional 4 h. Cytotoxicity was determined using an LDH cytotoxicity kit. Target cancer cells treated with 1% Triton X-100 for maximal LDH release were employed as a positive control and spontaneous LDH release from the untreated cells was used to subtract the background for each treatment. Upon completion of the treatment, 80 μL of supernatant of each treatment was mixed with 40 μL LDH detecting reagent in a new 96-well plate and the mixture was allowed for incubation for 30 min in dark at the incubator. Release of LDH was determined by following the manufacturers' instructions. The ADCC specific cell-killing was calculated through the following formula:

$$\text{ADCC\%} = \left(\frac{A_x - A_0}{A_{\text{max}}} \right) \times 100$$

' A_0 is the OD_{490} indicating the spontaneous LDH release from the effector cells control treatment; A_x is the OD_{490} from treatments of StxB-rhamnose conjugates or StxB protein in the presence of anti-rhamnose serum and PBMC; A_{max} is the OD_{490} indicating maximal LDH release from treatment with 1% Triton X-100.'

CDC Assay

The tumor killing capability of the StxB-rhamnose conjugates through CDC was determined by using HT29 as target cancer cells. HT29 cells ($10^4/\text{well}$) were seeded into 96 well-plate overnight. After removal of the supernatant, cells were then incubated with 200 μL of StxB-rhamnose conjugates (500 nM) or StxB protein (500 nM) in medium for 0.5 h. The supernatant was then removed and the cells were further incubated with 100 μL medium mixture of anti-rhamnose rabbit serum (1:50 dilution) and rabbit complement (2.5%, v/v). Negative control was achieved by replacing the conjugates with the same volume of PBS. Maximum cell-killing

control was performed by treating cells with 1% Triton X-100. After incubation at the cell culture incubator for 4 h, the cell viability was determined by using a WST-8 kit following the manufacturers' instructions. The CDC specific cell-killing was calculated through the following formula:

$$\text{CDC\%} = \left(1 - \frac{A_x - A_{\text{max}}}{A_0 - A_{\text{max}}}\right) \times 100$$

'A₀ is the OD₄₅₀ from treatment of PBS and anti-rhamnose serum; A_x is the OD₄₅₀ from treatments of StxB-rhamnose conjugates or StxB protein in the presence of anti-rhamnose serum; A_{max} is the OD₄₅₀ indicating the maximum cell-killing through treatment of 1% Triton X-100.'

Mice

All the mice used in this study were provided by Shanghai SLAC Laboratory Animal company and mice were grown in the animal center at Jiangnan university. All animal experiments in this work were conducted under the guidelines and protocols approved by the Institutional Animal Care and Use Committee of Jiangnan University [JN.No20210915b0 201201[316]].

Preparation of Mouse Anti-Rhamnose Serum

To obtain mouse serum containing anti-rhamnose antibodies for the therapeutic experiment, a vaccine conjugate of rhamnose and ovalbumin (OVA) was prepared by following the same procedure as we described early.²⁸ Balb/c mice were immunized with the rhamnose-OVA conjugate as reported previously.²⁹ Briefly, an emulsion was prepared by mixing the rhamnose-OVA conjugate (200 mg/mL) and alum adjuvant with a volume ratio of 1:1 (Sourav Sarkar, Steven A Lombardo et al. 2010). Each of total five mice (female, 6–8 weeks old) were injected with 100 μL of the emulsion subcutaneously (s.c.) at the abdomen on day 1, 7, 14 and 21. One week after the last immunization, mice were euthanized and whole blood was collected. The blood was then allowed to clot for 0.5 h at a fridge and serum was prepared by removing the clot through centrifugation at 2000 g for 15 min. The titer of rhamnose-specific antibody in serum was determined through a standard ELISA assay with HSA-Rhamnose immobilized on the plate.

In Vivo Anti-Tumor Efficacy in HT29 Xenograft Murine Model

The *in vivo* immunotherapy efficacy of the StxB-rhamnose conjugate against colorectal tumor was assessed in a HT29 xenograft murine model. To establish the mice model, Balb/c nude mice (6–8 weeks old, average weight 20 g/mouse) were subcutaneously (s.c.) implanted with 100 μL of HT29 cells (3 × 10⁶) in PBS at the abdominal right flanks. With growth for 6 days, mice with tumor volume of 40–70 mm³ were randomized into three groups (n=5) and the treatments for therapy were initiated on day 0 as illustrated in Fig. 6A. For the therapy effect of the StxB-rhamnose conjugate, mice (Group 1) were treated with 1B-3R conjugate (40 μg in 50 μL PBS) and anti-Rhamnose mouse serum (50 μL) through intravenous (i.v) injection at the tail vein. As parallel control groups, mice were treated with StxB protein (40 μg in 50 μL PBS, Group 2) or equivalent PBS (50 μL, group 3) in combination with anti-Rhamnose mouse serum (50 μL), respectively. All the treatments were given once a day for 6 days. The volume of tumor and mouse weight were measured every day for 12 days. Tumor length and width of each mouse were determined to calculate the volume of tumor using an equation as 1/2 × length × width². Upon completion of the therapy schedule, tumor tissue was dissected from the euthanized mice for measuring endpoint tumor weight. The tumor-growth-inhibition ability was

calculated by using the percentage of endpoint tumor weight reduction of StxB or 1B-3R treated group to tumor weight of the PBS treated control group. For the histological analysis of tumor tissue and major organs of mice after therapy, excised tumor, heart, liver, spleen, lung, and kidney were fixed using 10% neutral-buffered formalin solution. The sections of these tissues were stained with hematoxylin and eosin (HE) for assessment of morphological changes and images were recorded using a microscope.

Results

Construction and Characterization of StxB-Rhamnose Conjugates

In this study, we aimed to develop a multivalent antibody-recruiting molecule by conjugating the pentameric StxB protein with rhamnose modules. The crystal structure of shiga toxin indicates that the N terminus of its doughnut-shape StxB subunit is sterically close to its interaction interface with the Gb3 receptor expressed on the host cell surface, so it is reasonable to speculate that attaching an antibody-binding ligand at this site might affect Gb3 binding capability of the final construct (Fig. 1A).³⁰ However, the C terminus of StxB extends in an opposite direction away from the main protein structure, which made it feasible to place the rhamnose haptens at the C terminus of StxB to form a pentameric antibody-recruiting molecule (Fig. 1B). To this end, StxB of shiga toxin variant 1 and 2 were recombinantly prepared with a Myc tag, a Sortase A tag (LPTEG) and a 6xHis affinity tag fused at the C terminus (Fig. 1C and supporting Table 1). The rhamnose derivatives containing triple-glycine and polyethylene glycol (PEG) spacer were prepared as we described previously (Fig. 1C and supporting scheme S1).³¹ The recombinant StxB and rhamnose derivatives were conjugated together using a Sortase A-catalyzed site-specific ligation reaction (Fig. 1C). In the first step of the enzymatic reaction, Sortase A cleaved the peptide bond of Thr and Gly within the Sortase A tag, and then it formed a semi-stable thioacyl-intermediate with StxB protein through its active Cys. In the second step, the rhamnose derivatives as nucleophiles attacked the thioacyl bonds in the intermediates and formed a new peptide bond with StxB. As the His tag in StxB was enzymatically cleaved during the conjugation reaction, the final StxB-rhamnose conjugates can be reversely purified by removing unreacted proteins using magnetic nickel-beads. The excess rhamnose derivatives were further removed by a molecule weight cutting-off filter unit (3 kDa). The resultant conjugates were termed 1B-nR and 2B-nR (n = 1, 2, 3), where n stands for the number of PEG repeats. As shown in Fig. 1D, unrelated proteins were clearly removed and the StxB-rhamnose conjugates with high purity were identified on SDS-PAGE. The conjugates were further validated by western blotting analysis using anti-His tag, anti-Myc tag and anti-rhamnose antibodies, respectively (Fig. 1E). As we expected, His tag was not present among all the purified conjugates, while the Myc tag was detected throughout all the conjugates. Moreover, StxB-rhamnose conjugates except the parental StxB can be labeled by anti-rhamnose serum, therefore indicating its acquired capability of rhamnose antibody binding.

StxB-Rhamnose Conjugates Function as Pentamers

Because the pentameric format of StxB was reported to be required for its efficient binding to Gb3 receptor,^{32,33} we next determined whether the covalent addition of rhamnose affected the pentameric structure and Gb3 receptor-binding capability of the conjugates. The protein size distribution of the parental StxB and StxB-rhamnose was compared by using DLS (dynamic light scattering) analysis. As shown in Fig. 2A and 2B, the main portion of the conjugates maintained almost the same size as the parental proteins of around 100 nm in diameter. A small portion of the conjugates with a

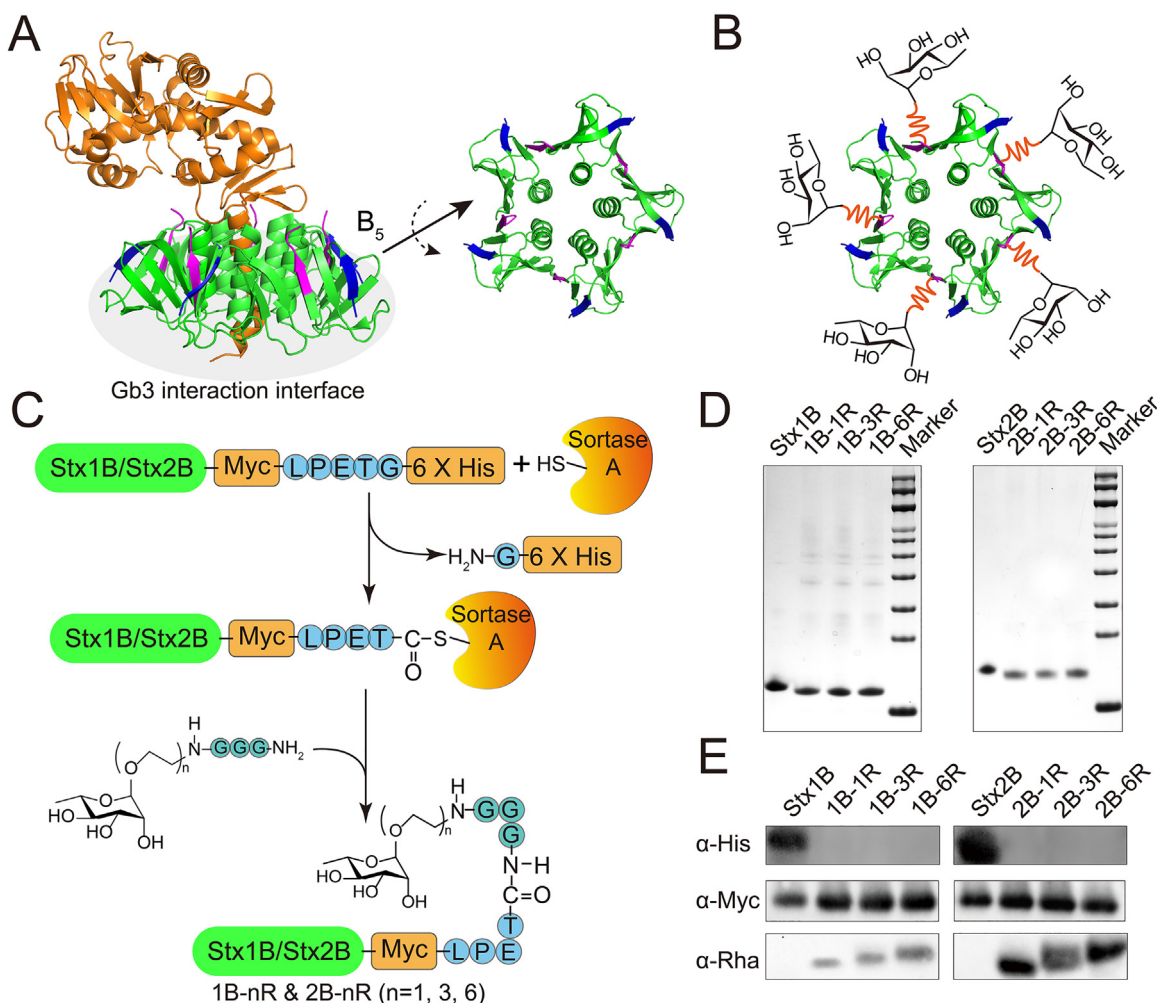


Figure 1. Construction and characterization of StxB-rhamnose conjugates. (A) The ribbon representation of Shiga toxin consisting of a subunit A, colored orange, and five subunits B, colored green (PDB: 6U3U). The C terminus of each subunit B is highlighted in magenta and the N terminus is highlighted in blue. (B) The model of rhamnose-conjugated StxB. Rhamnose is colored black and the PEG linker connecting rhamnose and the StxB is colored orange. (C) The schematic of the Sortase A-catalyzed site-specific conjugation of StxB with the rhamnosyl-lysine derivatives. (D) SDS PAGE analysis of the StxB-rhamnose conjugates. (E) Western blotting characterization of StxB-rhamnose conjugates using His tag, Myc tag and rhamnose antibodies, respectively. (For interpretation of the references to color in this figure legend, the reader is referred to the web version of this article.)

diameter around 20 nm was also detected, which matches the size of StxB monomers disassembled from the pentamer under acidic conditions (supporting figure S1). A very small portion of the conjugates 1B-6R, 2B-1R and 2B-6R seems to form aggregates, as indicated by the appearance of species with a diameter of around 5000 nm (Fig. 2A and 2B).

We further compared the Gb3 binding capability of the parental StxB with the related StxB-rhamnose conjugates, which was achieved by a Gb3-binding plate assay as we described previously.¹¹ As shown in Fig. 2C, all the StxB-rhamnose conjugates had the same binding capability to Gb3, although a significant decrease can be seen when compared to the parental StxB. As in shown in Fig. 2D, 2B-1R had the same capability as the parental StxB, but the 2B-3R and 2B-6R conjugates both showed a decreased capability similar to the StxB-rhamnose conjugates. Taken together, these data suggested that StxB conjugated with rhamnose maintained most of its pentameric constitution and the functional activity.

StxB-Rhamnose Conjugates Mediated Binding of Rhamnose Antibodies to Tumor Cells

We next determined the capability of these constructs to target cancer cells and mediate binding of anti-rhamnose antibodies *in vitro*.

In a scan of Gb3 expressing cells, colorectal cancer cell line HT29 showed the highest binding of Stx1B and Stx2B, and therefore it was used hereafter as the model of target cancer cells (Supporting Fig. S2). The binding capability of StxB-rhamnose conjugates to HT29 cells was first determined by using flow cytometry with anti-Myc primary antibodies and Alexa fluorescence labeled secondary antibodies. As shown in Fig. 3A and 3B, all the conjugates were able to bind potently to HT29 cells although a significant reduction of such capability was seen when it was compared with the parental Stx1B and Stx2B, which was consistent with the phenomenon as observed in the Gb3 binding plate assay (Fig. 2C and 2D). Although those conjugates with the same StxB scaffold displayed almost the same binding capability to Gb3, it still can't exclude the possibility that the linker connecting the StxB and rhamnose moiety may affect its ability to bind rhamnose antibodies. Thus, the antibody-recruiting capability of StxB-rhamnose conjugates was further determined using flow cytometry with anti-rhamnose rabbit serum. As shown in Fig. 3C and D, all the conjugates were able to efficiently direct rhamnose antibodies onto HT29 tumor cells. Among the StxB-based conjugates 1B-6R showed the most potent antibody-recruiting capability while all the StxB-based conjugates showed similar activity. In general, the StxB-based conjugates showed higher antibody binding capability than those based on Stx1B, which might be caused by its higher Gb3 binding affinity. In

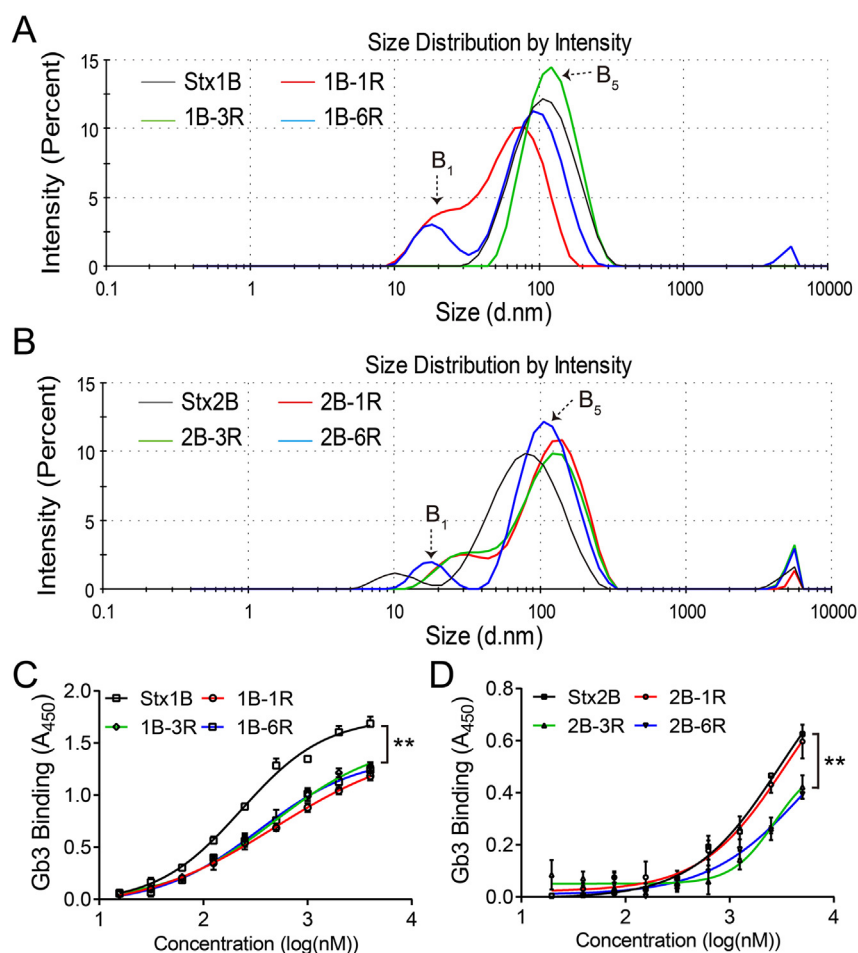


Figure 2. StxB-rhamnose conjugates function as pentamers. (A) DLS analysis of StxB and the corresponding conjugates. B₁ indicates the monomer StxB and B₅ indicates the pentamer StxB. Comparison of Gb3 binding capability of StxB₁B (C) or StxB₂B (D) with the corresponding conjugates through a Gb3 binding plate assay (**: $p < 0.01$).

addition, the binding of rhamnose antibodies was further visualized by an immunocytochemistry assay using anti-rhamnose rabbit serum and the results generally corresponded well with the observed antibody binding by flow cytometry analysis (Fig. 4). All StxB-rhamnose conjugates were capable of directing rhamnose antibodies binding onto the surface of HT29 cells, while no significant fluorescence signal was observed in the parental StxB₁B or StxB₂B treated HT29 cells.

StxB-Rhamnose Conjugates Killed Tumor Cells Through ADCC and CDC

As the conjugates can efficiently direct rhamnose antibodies onto HT29 cancer cells, we then assessed their ability to kill tumor cells through antibody-dependent immune effector functions, including ADCC and CDC (Fig. 5A). To determine the ADCC effect, HT29 cells as the target cancer cells were first treated by the parental StxB₁B and StxB₂B as the negative control or the corresponding StxB-rhamnose conjugates in the presence of rabbit serum containing rhamnose antibodies, and then all the cells were incubated with human PBMC isolated from blood of healthy donors as effector immune cells. Target cancer cell lysis was determined by an LDH (lactate dehydrogenase) test. As shown in Fig. 5B, StxB₁B itself showed 10% cytotoxicity and StxB₂B itself showed 24% cytotoxicity against HT29 cells, which were not dependent on the PBMC related cytotoxicity (Supporting Figure S3). All the StxB₁B-based conjugates showed a similar cytotoxicity of 40% cell lysis. Among the StxB₂B-based conjugates, 2B-1R and 2B-6R caused ca. 36% cell lysis, while the 2B-3R showed the best of cell lysis

ratio of ca. 46%. To determine the CDC effect, HT29 cells were first treated with conjugates and the rhamnose antibody serum same as above for ADCC assay, and the treated cells were further incubated with the rabbit complement instead of effector immune cells (Fig. 5C). The target cancer cell viability was tested by using a WST-8 kit. Consistent with the ADCC, the StxB₁B and StxB₂B parental proteins showed a basal cell lysis of 14% and 34%, respectively. All the conjugates showed cell lysis of over 40% and the 1B-3R and 2B-3R showed the highest potency of 67% and 78% in their respective subgroup. This specific cytotoxicity of ADCC and CDC was also observed in Hela cancer cells which showed high Gb3 expression (Supporting Fig. S4). In addition, the effect of the conjugate on a normal colon mucosa cell line NCM460 was determined to assess possible off-target toxicity. As expected, the 1B-3R conjugate did not show significant ADCC and CDC cytotoxicity in NCM460 cells (Supporting Fig. S5), although the parental StxB proteins had moderate direct toxicity (Supporting Fig. S6). As a higher basal cytotoxicity of StxB₂B was observed, the most potent conjugate with the StxB₁B scaffold, *i.e.* 1B-3R, was chosen for further therapeutic studies.

1B-3R Conjugate Suppressed Tumor Growth in HT29 Xenograft Tumor Murine Model

Finally, the capability of 1B-3R conjugate to inhibit tumor growth was determined in a colorectal tumor xenograft murine model. HT29 cells were implanted subcutaneously into the abdominal right flanks

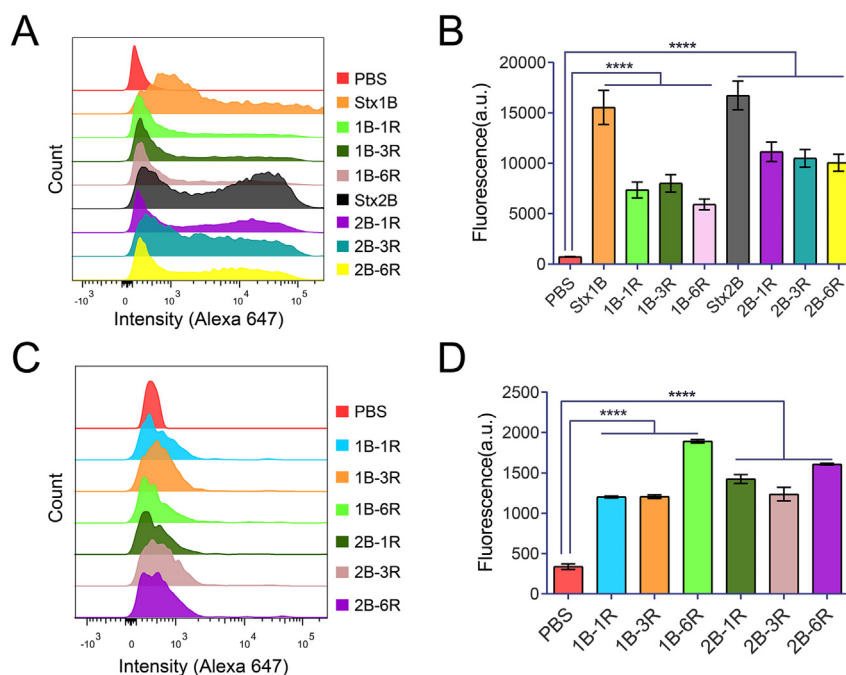


Figure 3. Flow cytometry analysis of StxB-rhamnose conjugates mediated recruitment of rhamnose antibody. HT29 cells were treated with the parental StxB or the conjugates at a concentration of 500 nM. The binding of the conjugates to HT29 cells were determined by Flow cytometry using anti-Myc rabbit IgG antibodies and Alexa Fluor 647-labeled Goat Anti-Rabbit IgG antibodies (A), while the recruitment of rhamnose antibody was determined using anti-rhamnose rabbit serum and Alexa Fluor 647-labeled Goat Anti-Rabbit IgG antibodies (C). (B) and (D) are the corresponding mean fluorescence intensity (MFI) quantification of (A) and (C), respectively (****: $p < 0.0001$). PBS was used as a negative control.

of Balb/c nude mice and mice with a palpable tumor (size 50–70 mm³) were randomized into three groups (5 mice/group) for the treatment. As the tumor-bearing murine model does not contain circulating anti-rhamnose antibodies, such therapeutic evaluations were often achieved by injecting the drug candidates simultaneously with mouse serum containing the hapten antibodies. For this reason, mouse serum with high titer of rhamnose-specific antibody was obtained through immunization of Balb/c mice by OVA-rhamnose conjugates (Fig. 6A and Supporting Fig. S7). As shown by the therapy schedule in Fig. 6A, one group of tumor-bearing mice was treated with 1B-3R conjugate in combination with the rhamnose antibody-containing serum through intravenous injection once a day for six days and parallel controls were set up by replacing 1B-3R with PBS or Stx1B protein. As we expected, the xenograft tumor growth was profoundly slowed down in the group of mice treated with the 1B-3R conjugate, while the parental protein Stx1B had no inhibitory effect on the tumor growth (Fig. 6B). The endpoint tumor size and tumor weight of mice treated with 1B-3R were significantly less than that of mice treated with the parental Stx1B protein and PBS vehicle (Fig. 6C and D), and the general tumor-growth-inhibition (TGI) rate of 1B-3R was ca. 49% (Fig. 6E). Like the vehicle control, both the treatments of Stx1B and 1B-3R conjugate were generally safe, as no remarkable changes in the body weight of all the tumor-bearing mice were observed throughout the therapeutic course (Supporting Fig. S8). We further assessed the anticancer effect and safety of the conjugate by histological analysis of tumor tissues and major organs with HE staining. As shown in Fig. 7, the staining indicated clear apoptosis in tumor tissue from 1B-3R treated mice, and there was obviously lower cancer cell density than that from both PBS and Stx1B treated mice. As we expected, no significant morphologic changes were seen in heart, liver, spleen, lung, kidney, indicating that both the Stx1B protein and the 1B-3R conjugate did not induce obvious systemic toxicity. Taken together, those data suggest that the 1B-3R conjugate is a potential antibody-recruiting chimera for the Gb3-targeted immunotherapy of colorectal cancer.

Discussion

Cancer immunotherapy is a type of targeted-cancer treatment that manipulates or utilizes the immune regulatory mechanisms to fight cancer, which offers substantial benefits over the traditional therapeutic options such as enhanced specificity and long-term cancer suppression. Over recent years, tremendous immunotherapies have been developed for cancer treatment and significant clinical benefits of immunotherapy have been seen, especially for those of immune checkpoint inhibitors and engineered-immune cells. However, due to the highly heterogeneous nature of cancer, more effective immunotherapy approaches are still required for certain types of cancer. In addition, the complexity of immunotherapy inevitably increases the cost of such treatment and therefore practical options are also favored.

Antibody-recruiting molecule is a novel type of passive cancer immunotherapy. Antibody-recruiting molecules recognize the tumor cells and signal the antibodies existing naturally in the human blood to attack the tumor. We herein developed a multivalent antibody-recruiting chimera consisting of StxB conjugated with the rhamnose hapten for Gb3-targeted immunotherapy of colorectal cancer, taking advantage of its natural pentameric architecture and Gb3-specific recognition. Multivalency in an antibody-recruiting molecule has been demonstrated by using scaffold of liposomes, lipid polymers, glycopolymers, peptide scaffolds and synthetic clusters,^{21–25,34} but these approaches mostly require tedious chemical synthesis and complicated characterization of the molecules. We demonstrated that StxB-based antibody-recruiting molecule can be efficiently prepared through a practical enzymatic approach and it showed potent antitumor activity although the binding affinity dropped moderately after conjugation. Taking into account its economical production and excellent stability, StxB should be a favorable scaffold to develop such multivalent therapeutics targeting the Gb3 receptor.

StxB was reported to be quickly endocytosed by cells upon binding to the Gb3 receptor,⁵ which might compromise the binding of the rhamnose antibody to the target cancer cells and therefore decrease

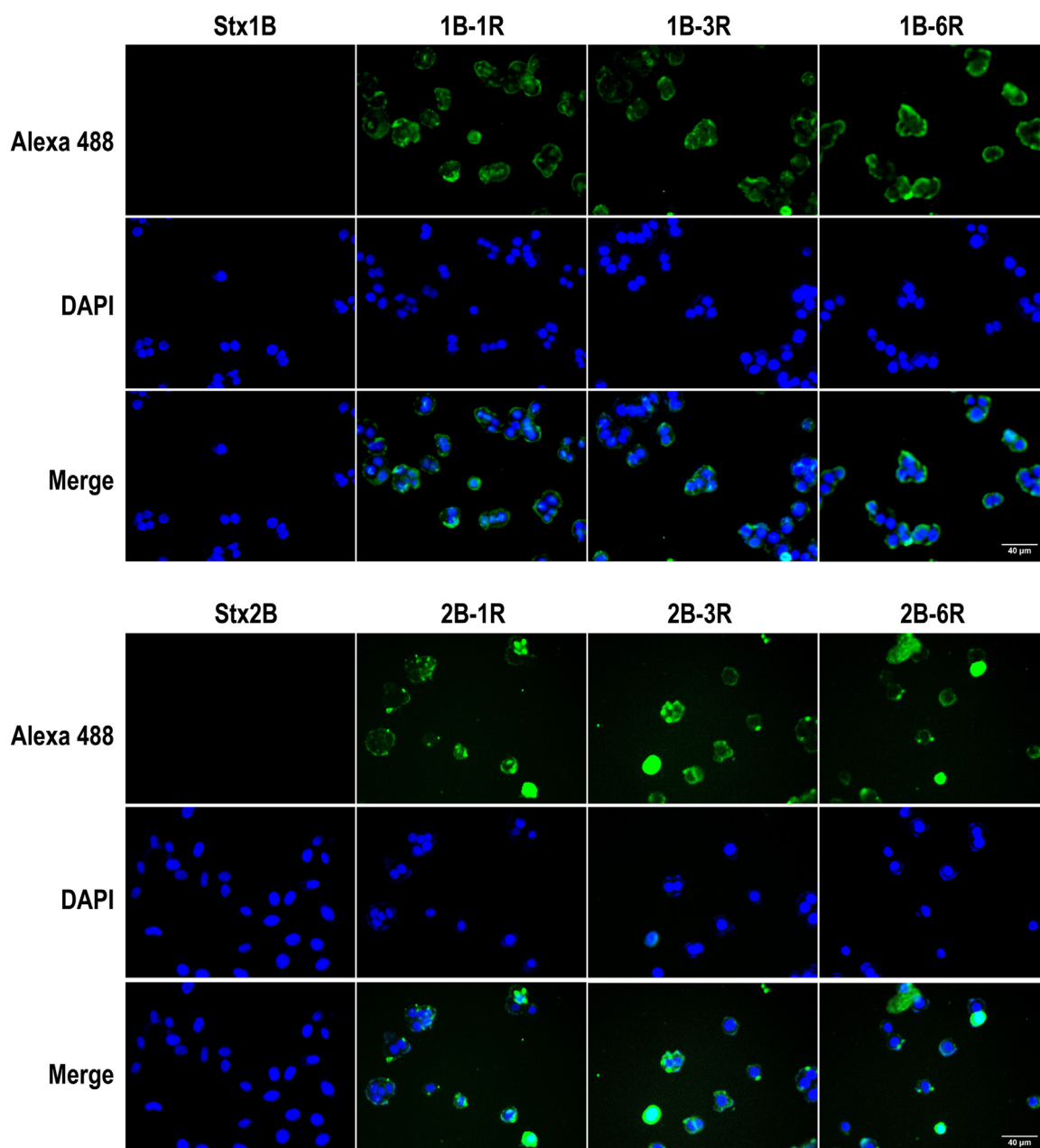


Figure 4. Immunocytochemistry analysis of StxB-rhamnose conjugates mediated antibody binding. HT29 cells were incubated with StxB-rhamnose conjugates or StxB proteins at 500 nM, followed by anti-rhamnose rabbit serum. The binding of rhamnose antibodies to the cells was observed under fluorescent microscopy by using Alexa Fluor 488-labeled Goat Anti-Rabbit IgG antibodies.

the expected antitumor efficacy. However, despite these StxB-rhamnose conjugates were preincubated with the cells prior to the addition of the rhamnose antibody in our *in vitro* analysis, the rhamnose antibody could still efficiently bind to target cells (Fig. 3D) and mediate potent tumor cell killing (Fig. 5C). This can be due to the fact that different types of cell lines showed variable StxB uptake kinetics and the conjugates can't be completely endocytosed in a short time. Additionally, the rhamnose conjugation with a PEG spacer might also have a small chance to influence the StxB uptake kinetics. These determining factors on the StxB uptake can be carefully studied to further improve the efficacy by reducing the endocytosis of the conjugates.

Although remarkable clinical success has been achieved in the immunotherapy of hematologic tumors, most of current immunotherapy approaches showed compromised efficacy in solid tumors.^{35–37} Interestingly, our *in vivo* evaluation of StxB-rhamnose conjugate

(1B-3R) showed that it can significantly decrease the tumor size with a tumor-growth inhibition rate of ca. 49%. It has been suggested that increasing the dose of antibodies can improve the antibody-based therapy of solid tumor.³⁸ Thus, we speculated that the StxB-rhamnose conjugate might be able to concentrate antibodies onto the tumor cells through the potential multivalent effect enabled by the multiple rhamnose haptens from the conjugates. Therefore, an enhanced tumor elimination is conceivable. Moreover, the high selectivity of the Gb3 receptor binding enabled by the multivalent StxB structure might also contribute to the promising antitumor activity. Further investigations should be carried out to explore the mechanisms.

Taken together, our results demonstrated that StxB-rhamnose conjugates are capable as multivalent antibody-recruiting molecules of modulating the innate immune effectors to attack tumor cells *in vitro* and *in vivo*, rendering this kind of construct as an excellent

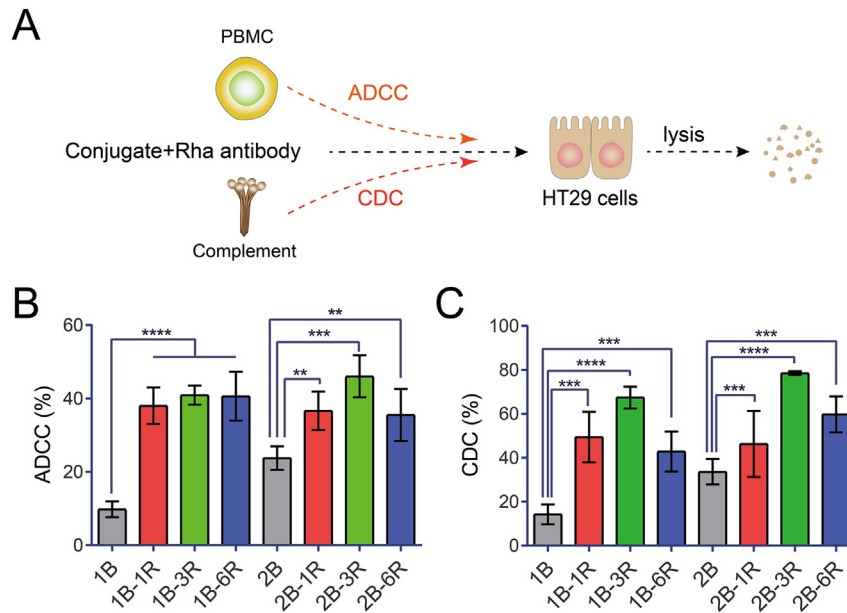


Figure 5. StxB-rhamnose conjugates induce lysis of HT29 cancer cells through immune effector functions. (A) Schematic of ADCC and CDC assay. ADCC-specific cytotoxicity (B) and CDC-specific cytotoxicity (C) against HT29 cells (**: $p < 0.01$, ***: $p < 0.001$, ****: $p < 0.0001$).

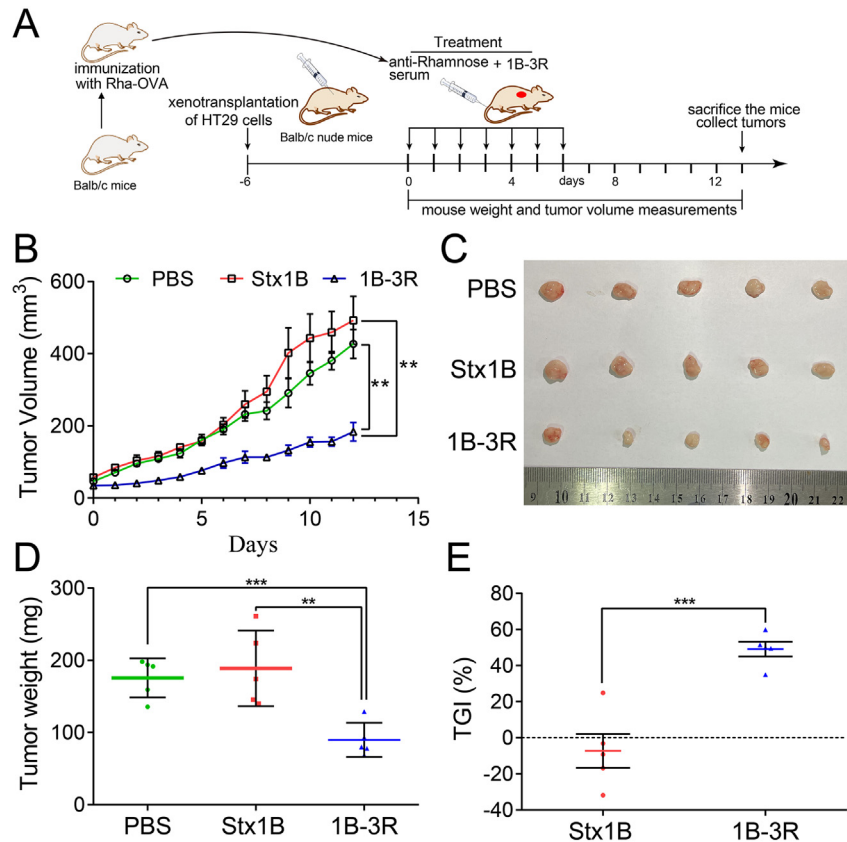


Figure 6. Therapeutic efficacy of 1B-3R conjugate against colorectal cancer in the HT29 xenograft tumor murine model. (A) Schematic of the Balb/c mice immunization with Rhamnose-OVA and therapy schedule of tumor-bearing Balb/c nude mice with the 1B-3R conjugate. (B) The average tumor volume of mice from each treated group. (C) The images of endpoint tumor collected from each treated mouse. (D) The endpoint tumor weight of mice. (E) The average tumor growth inhibition (TGI) rates of 1B-3R conjugate and Stx1B were determined by the reduction percentage of tumor weight with respect to the tumor weight of PBS-treated mice (**: $p < 0.01$, ***: $p < 0.001$, ****: $p < 0.0001$).

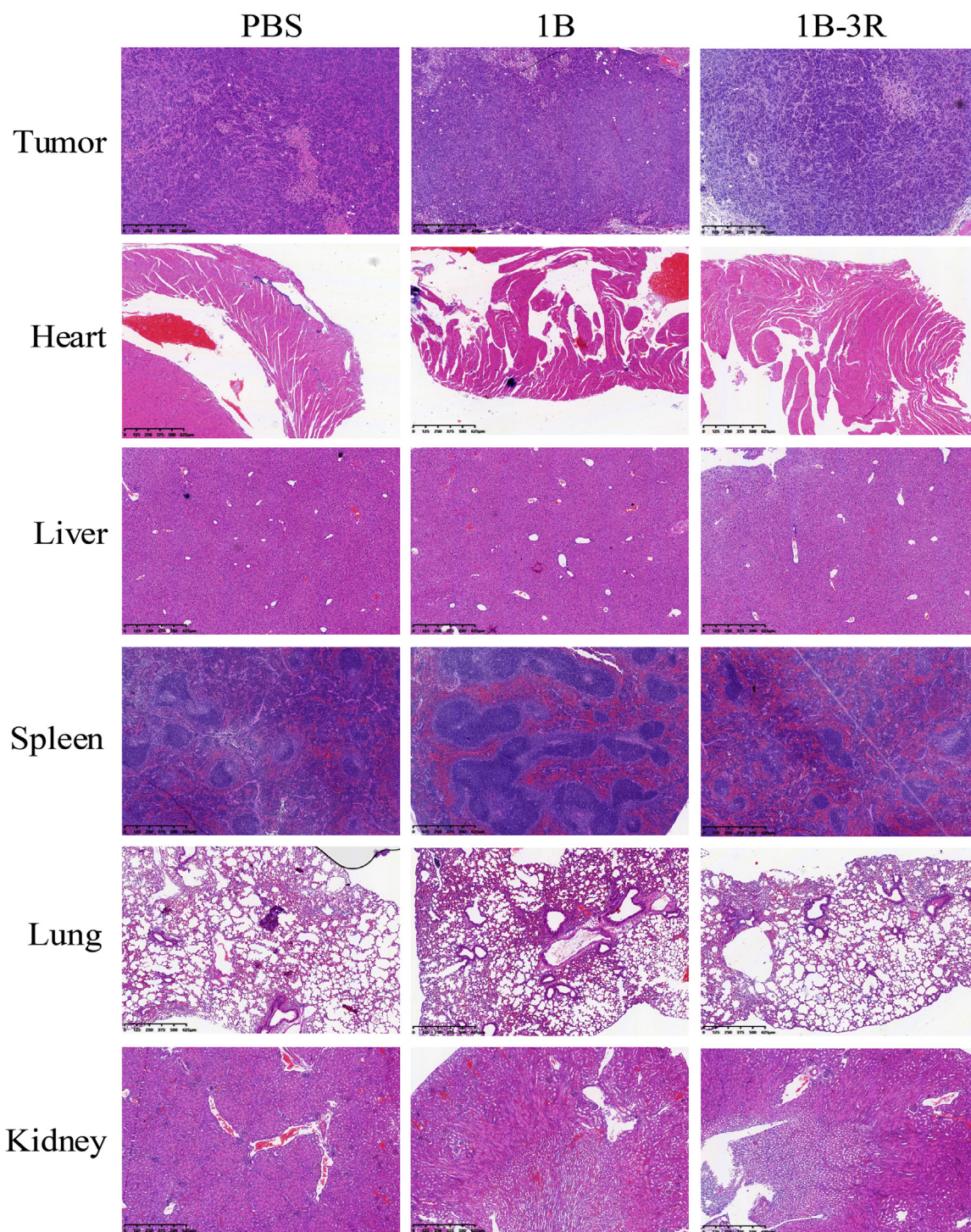


Figure 7. Histological analysis of tumor tissue and major organs. Sections of tumor tissue, heart, liver, spleen, lung and kidney from treated mice were assessed with HE staining.

candidate for Gb3-targeted immunotherapy of colorectal cancer. Definitely, additional investigations remain required to validate the tumor-specificity of these constructs, as Gb3 receptor is also commonly expressed on other types of normal cells.

Conclusion

The development of Gb3 receptor-targeted cancer therapeutics has been challenging. In the present work, we constructed a novel bioconjugate consisting of StxB lectin and rhamnose hapten as an

endogenous antibody-recruiting chimera for Gb3-targeted immunotherapy of colorectal cancer, by taking advantage of the Gb3-specific binding and the natural pentameric architecture of StxB protein. The site-specific conjugation of rhamnose moieties at the C terminus of StxB was achieved through an efficient Sortase A-catalyzed enzymatic approach and StxB-rhamnose conjugates kept the pentamer architecture as well as the ability to bind to Gb3 receptor expressed on HT29 colorectal cancer cells. All the constructs were capable of efficiently mediating the binding of rhamnose antibodies onto HT29 cancer cells and eliciting strong ADCC and CDC-specific cytotoxicity

against HT29 cancer cells *in vitro*. One of the conjugates, *i.e.* 1B–3R, was confirmed to be able to suppress the colorectal tumor growth using a murine xenograft tumor model. Our results demonstrated the potential use of StxB as an excellent multivalent scaffold to develop antibody-recruiting construct or similar multivalent therapeutics against cancer, although more are needed to further improve its pharmaceutical properties.

Declaration of Competing Interest

None.

Acknowledgments

This work was supported by the National Natural Science Foundation of China [No. 21907038 and No. 32000904]; Health and Family planning Commission of Wuxi, China [No. Z202005]; Natural Science Foundation of Jiangsu Province [No. BK20200601]; China Postdoctoral Science Foundation [No. BX20200153 and No. 2021M691293]; and the 111 Project [No. 111-2-06]. J. Shi was also supported by the basic research program of Jiangnan university [No. JURP12016] and the innovation and entrepreneurship program of Jiangsu province, China.

Supplementary Materials

Supplementary material associated with this article can be found in the online version at doi:10.1016/j.xphs.2022.07.017.

References

- Bien T, Perl M, Machmuller AC, et al. MALDI-2 mass spectrometry and immunohistochemistry imaging of Gb3Cer, Gb4Cer, and further glycosphingolipids in human colorectal cancer tissue. *Anal Chem*. 2020;92(10):7096–7105.
- Distler U, Souady J, Hulsewig M, et al. Shiga toxin receptor Gb3Cer/CD77: tumor-association and promising therapeutic target in pancreas and colon cancer. *PLoS One*. 2009;4(8):e6813.
- Falguieres T, Maak M, von Weyhern C, et al. Human colorectal tumors and metastases express Gb3 and can be targeted by an intestinal pathogen-based delivery tool. *Mol Cancer Ther*. 2008;7(8):2498–2508.
- Geyer PE, Maak M, Nitsche U, et al. Gastric adenocarcinomas express the glycosphingolipid Gb3/CD77: targeting of gastric cancer cells with Shiga toxin B-subunit. *Mol Cancer Ther*. 2016;15(5):1008–1017.
- Maak M, Nitsche U, Keller L, et al. Tumor-specific targeting of pancreatic cancer with Shiga toxin B-subunit. *Mol Cancer Ther*. 2011;10(10):1918–1928.
- Stimmer L, Dehay S, Nemati F, Massonnet G, Richon S, Decaudin D, Klijanienko J, Johannes L. Human breast cancer and lymph node metastases express Gb3 and can be targeted by STxB-vectorized chemotherapeutic compounds. *BMC Cancer*. 2014;14:916.
- Desselle A, Chaumette T, Gaugler MH, et al. Anti-Gb3 monoclonal antibody inhibits angiogenesis and tumor development. *PLoS One*. 2012;7(11):e45423.
- Kondo Y, Tokuda N, Furukawa K, et al. Efficient generation of useful monoclonal antibodies reactive with globotriaosylceramide using knockout mice lacking Gb3/CD77 synthase. *Glycoconj J*. 2011;28(6):371–384.
- Haji-Ghassemi O, Blackler RJ, Martin Young N, Evans SV. Antibody recognition of carbohydrate epitopes dagger. *Glycobiology*. 2015;25(9):920–952.
- Melton-Celsa AR. Shiga toxin (Stx) classification, structure, and function. *Microbiol Spectr*. 2014;2(4). EHEC-0024-2013.
- Haksar D, Asadpoor M, Heise T, et al. Fighting shigella by blocking its disease-causing toxin. *J Med Chem*. 2021;64(9):6059–6069.
- Kim M, Binnington B, Sakac D, et al. Comparison of detection methods for cell surface globotriaosylceramide. *J Immunol Methods*. 2011;371(1–2):48–60.
- Batiste C, Dransart E, Ait Sarkouh R, et al. A new delivery system for auristatin in STxB-drug conjugate therapy. *Eur J Med Chem*. 2015;95:483–491.
- Mohseni Z, Sedighian H, Halabian R, Amani J, Behzadi E, Imani Fooladi AA. Potent *in vitro* antitumor activity of B-subunit of Shiga toxin conjugated to the diphtheria toxin against breast cancer. *Eur J Pharmacol*. 2021;899:174057.
- Kostova V, Dransart E, Azoulay M, et al. Targeted Shiga toxin-drug conjugates prepared via Cu-free click chemistry. *Bioorg Med Chem*. 2015;23(22):7150–7157.
- Couture O, Dransart E, Dehay S, Nemati F, Decaudin D, Johannes L, Tanter M. Tumor delivery of ultrasound contrast agents using Shiga toxin B subunit. *Mol Imaging*. 2011;10(2):135–143.
- Ehrenfeld M, Schrade A, Flisikowska T, et al. Tumor targeting with bacterial Shiga toxin B-subunit in genetic porcine models for colorectal cancer and osteosarcoma. *Mol Cancer Ther*. 2022;21(4):686–699.
- Liu J, Hong H, Shi J, et al. Dinitrophenol-mediated modulation of an anti-PD-L1 VHH for Fc-dependent effector functions and prolonged serum half-life. *Eur J Pharm Sci*. 2021;165:105941.
- Achilli S, Berthet N, Renaudet O. Antibody recruiting molecules (ARMs): synthetic immunotherapeutics to fight cancer. *RSC Chem Biol*. 2021;2(3):713–724.
- Uvyn A, De Geest BG. Multivalent antibody-recruiting macromolecules: linking increased binding affinity with enhanced innate immune killing. *ChemBioChem*. 2020;21(21):3036–3043.
- Li X, Rao X, Cai L, et al. Targeting Tumor cells by natural anti-carbohydrate antibodies using rhamnose-functionalized liposomes. *ACS Chem Biol*. 2016;11(5):1205–1209.
- Uvyn A, De Coen R, Gruijs M, et al. Efficient innate immune killing of cancer cells triggered by cell-surface anchoring of multivalent antibody-recruiting polymers. *Angew Chem Int Ed Engl*. 2019;58(37):12988–12993.
- De Coen R, Nuhn L, Perera C, et al. Synthetic rhamnose glycopolymer cell-surface receptor for endogenous antibody recruitment. *Biomacromolecules*. 2020;21(2):793–802.
- Lin H, Zhou K, Li D, et al. Dinitrophenol-hyaluronan conjugates as multivalent antibody-recruiting glycopolymers for targeted cancer immunotherapy. *ChemMedChem*. 2021;16(19):2960–2968.
- Liet B, Laigre E, Goyard D, et al. Multifunctional glycoconjugates for recruiting natural antibodies against cancer cells. *Chemistry*. 2019;25(68):15508–15515.
- Hong H, Zhou Z, Zhou K, Liu S, Guo Z, Wu Z. Site-specific C-terminal dinitrophenylation to reconstitute the antibody Fc functions for nanobodies. *Chem Sci*. 2019;10(40):9331–9338.
- Shin IS, Nishikawa K, Maruyama H, Ishii S. Histidine-tagged shiga toxin B subunit binding assay: simple and specific determination of gb3 content in mammalian cells. *Chem Pharm Bull (Tokyo)*. 2006;54(4):522–527.
- Lin H, Hong H, Wang J, Li C, Zhou Z, Wu Z. Rhamnose modified bovine serum albumin as a carrier protein promotes the immune response against sTn antigen. *Chem Commun (Camb)*. 2020;56(90):13959–13962.
- Sarkar S, Lombardo SA, Herner DN, Talan RS, Wall KA, Sucheck SJ. Synthesis of a single-molecule L-rhamnose-containing three-component vaccine and evaluation of antigenicity in the presence of anti-L-rhamnose antibodies. *J Am Chem Soc*. 2010;132(48):17236–17246.
- Hughes AC, Zhang Y, Bai X, et al. Structural and functional characterization of Stx2k, a new subtype of Shiga toxin 2. *Microorganisms*. 2020;8(1):4.
- Li C, Dai SJ, Cao AJ, Zhou ZF, Wu ZM. Design and synthesis of rhamnose-modified exenatide conjugate by sortase A-mediated ligation. *J Carbohydr Chem*. 2019;38(3):167–178.
- Solytk AM, MacKenzie CR, Wolski VM, et al. A mutational analysis of the globotriaosylceramide-binding sites of verotoxin VT1. *J Biol Chem*. 2002;277(7):5351–5359.
- Zhang J, Tanha J, Hiramata T, et al. Pentamerization of single-domain antibodies from phage libraries: a novel strategy for the rapid generation of high-avidity antibody reagents. *J Mol Biol*. 2004;335(1):49–56.
- Ou C, Prabhu SK, Zhang X, Zong G, Yang Q, Wang LX. Synthetic antibody-rhamnose cluster conjugates show potent complement-dependent cell killing by recruiting natural antibodies. *Chemistry*. 2022;28(16):e202200146.
- Taefehshokr S, Parhizkar A, Hayati S, et al. Cancer immunotherapy: challenges and limitations. *Pathol Res Pract*. 2022;229:153723.
- Fernandez de Larrea C, Staehr M, Lopez AV, et al. Defining an optimal dual-targeted CAR T-cell therapy approach simultaneously targeting BCMA and GPRC5D to prevent BCMA escape-driven relapse in multiple myeloma. *Blood Cancer Discov*. 2020;1(2):146–154.
- van de Donk N, Themeli M, Usmani SZ. Determinants of response and mechanisms of resistance of CAR T-cell therapy in multiple myeloma. *Blood Cancer Discov*. 2021;2(4):302–318.
- Cruz E, Kayser V. Monoclonal antibody therapy of solid tumors: clinical limitations and novel strategies to enhance treatment efficacy. *Biologics*. 2019;13:33–51.